ACS APPLIED MATERIALS & INTERFACES

Research Article

www.acsami.org

Stiff Diamond/Buckypaper Carbon Hybrids

T. Holz,*[,†] D. Mata,[†] N. F. Santos,[†] I. Bdikin,[‡] A. J. S. Fernandes,[†] and F. M. Costa[†]

[†]I3N, Physics Department, University of Aveiro, Campus de Santiago, 3810-193, Aveiro, Portugal

[‡]TEMA-NRD, Mechanical Engineering Department, Aveiro Institute of Nanotechnology (AIN), University of Aveiro, Campus de Santiago, 3810-193, Aveiro, Portugal

Supporting Information

ABSTRACT: Given the specific properties of each carbon allotrope such as high electrical/thermal conductivity of multiwall carbon nanotubes (MWCNT) and extreme hardness and high inertness of nanocrystalline diamond (NCD), the integration of both carbon phases is highly desirable. Therefore, in the present work, buckypapers were produced from MWCNT suspensions and were used as free-standing substrates to be coated with NCD by microwave plasma chemical vapor deposition (MPCVD). The integration of both allotropes was successfully achieved, the CNTs being preserved after diamond growth as confirmed by μ-Raman spectroscopy and scanning electron microscopy (SEM). Additionally, a good linkage was observed, the CNTs remaining embedded within the NCD matrix, thus reinforcing the interface of the resulting hybrid structure. This was corroborated by bending tests in a modified nanohardness tester. The increase of the Young's modulus from 0.3 to 300 GPa after NCD growth enables the use of this material in a wide range of applications including microelectromechanical systems (MEMS). Additionally, a highly anisotropic electrical resistivity behavior was confirmed: low in-plane values were found for the CNT layer (1.39×10^{-2} Ω.cm), while high transverse ones were measured for both the NCD coated and uncoated CNT buckypapers (8.13×10^{5} and 6.18×10^{2} Ω.cm, respectively).

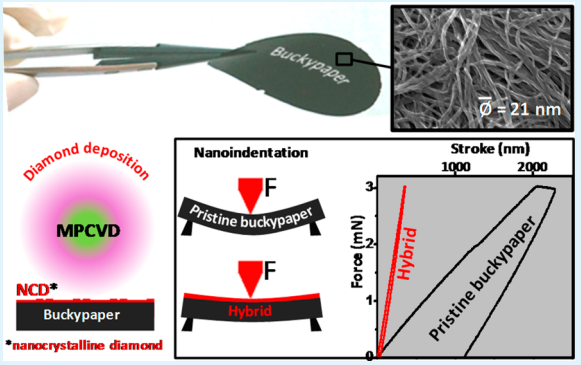

KEYWORDS: *MWCNT, buckypaper, diamond, CVD, nanoindentation*

1. INTRODUCTION

Almost five decades have passed since the onset of the enthusiasm for carbon allotropes, earlier with the well-known 3D sp^2/sp^3-hybridized graphite/diamond phases and, more recently, with non-3D sp^2 carbon clusters of a few atoms able to yield highly stable closed cage nanostructures, fullerenes (0D) and carbon nanotubes (1D), or open nanostructures—cones (0D), graphene (2D), and ribbons (2D)—accountable for triggering the nanoscience and nanotechnology revolution worldwide.[1] Individually, each carbon structure presents singular properties because of the type of hybridization, size scale, and spatial arrangement that yield exciting technological applications, currently under intense research.[2]

Recent works emphasize a well-outlined roadmap for these carbon forms focusing the combination of different nanosized allotropes to explore the best properties of each individual phase.[3−5] One example is the nanocrystalline diamond (NCD) and carbon nanotube (CNT) composites, potentially combining the extreme hardness/inertness and good thermal conductivity of the former with the high toughness and electrical conductivity of the latter. Nevertheless, some speculation remains about the properties that can be attained in these CNT/NCD composites because the translation of the properties of each individual phase into a hybrid material, including either monolithic or multilayered, is not straightforward.[4,6,7] Therefore, to achieve better control on the properties of this new class of materials, it becomes mandatory to perform exhaustive synthesis studies on the conditions that rule the coexistence of both phases.

Several attempts have been reported of chemical vapor deposition (CVD) synthesis of CNT/NCD hybrids using different approaches. In particular, Fernandes et al. presented a simultaneous microwave plasma chemical vapor deposition (MPCVD) synthesis of NCD and CNTs on Si substrates using an Fe bed as catalyst with metallic particles being continuously delivered by a diffusion/codeposition mechanism.[8] Another single-step method was developed by Varshney et al. to fabricate CNT/diamond composite films by hot filament chemical vapor deposition (HFCVD) on copper substrates coated with paraffin wax used as a seeding material for both carbon phases.[9] Despite the augmented interfacing properties between the two carbon forms, yielded by these one-step simultaneous growth methods, it is truly challenging to define the processing parameter window for their coproduction and preservation.

Received: October 2, 2014
Accepted: November 20, 2014
Published: November 20, 2014

Unlike single-step methods, CNT/NCD hybrids can be prepared by simple multistep processes. For example, CNTs are CVD grown on Si or metallic substrates precoated with a CVD diamond film decorated with catalytic metal particles, therefore nucleating and growing the tube structures.[7,10] In these studies, the CNTs are grown by the so-called base growth method where the metal catalyst particles remain attached to the diamond surface because of strong CNT/diamond adhesion forces.[11,12] Disadvantageously, the remaining metal particles in the final multilayer composite structure may negatively affect their electromechanical properties.[11]

Alternative catalyst-free methods, yet less commonly used, applying an upside-down approach with CNTs now acting as substrates have also been considered.[12] In that approach, nanoparticles of diamond, the nucleation sites for NCD, were dispersed on a CNT film precasted by spin coating on a Si substrate. One disadvantage of this method concerns the topographic irregularities of the CNT film surface that restrict the uniformity and full closing of the upper diamond film.[12] Nevertheless, highly dense uniform CNT films, also known as buckypapers, can be obtained by vacuum filtration with tailored thickness and CNT−CNT packing and alignment levels.[13] For these reasons, free-standing CNT buckypapers become promising substrates to prepare CNT/NCD hybrids. Yet, studies investigating the use of these nanotemplates are limited, with only one report being available to our knowledge. In this paper, it is claimed that vacuum-filtered Singlewall Carbon Nanotube (SWCNT) buckypapers yield uniform CNT/NCD constructs, but electrical and mechanical data were neglected.[14] Nevertheless, it might be anticipated that these hybrid buckypapers should present mechanical, thermal, and electrical properties of great interest for high-tech applications such as thermal management of integrated circuits, field emission devices, and, particularly, in nano- and microelectromechanical systems (NEMS\MEMS) with enhanced electrical field shielding.[15] Specifically, NCD films keep many of the outstanding intrinsic diamond properties relevant for applications in MEMS, namely, their stiffness and low intrinsic energy losses, far exceeding those of the traditionally used materials, particularly silicon.[16,17] Therefore, the integration of NCD with CNTs in the form of buckypaper membranes may be suitable for these applications as long as their mechanical properties are adequate.

The present work focuses on the preparation route and characterization of CNT/NCD hybrids. Free-standing CNT buckypapers were used as substrates for subsequent MPCVD growth studies of NCD films on one side of the paper. The phase composition and morphology of the staked films and interfaces were thoroughly evaluated by μ-Raman spectroscopy and scanning electron microscopy (SEM), with the CNTs preservation and intercalation with the NCD film being discussed. The Young's modulus of the NCD coated structures was assessed by bending tests in a modified nanoindentation system to evaluate their potential to be integrated in MEMS. The correlation between the hybrid morphology/structure and the mechanical behavior is also discussed.

2. EXPERIMENTAL SECTION

2.1. CNT Buckypaper Production. Functionalized multiwalled carbon nanotubes (Nanocyl, NC3101), with a purity level of 95 wt % and a 4 wt % content of covalently bonded carboxylic groups (−COOH), were used to prepare the CNT buckypapers.

CNT buckypapers mixed with diamond particles in a weight ratio of 2:1 were prepared in isopropyl alcohol (IPA, ≥99.8%, Sigma-Aldrich) following six main steps.[18] (1) CNT suspensions of 1 g L^{-1} were dispersed by high-speed shearing for 30 min (IKA T25-Ultra-Turrax, 20 500 rpm) with a shear force of 96 Pa to eliminate big CNT agglomerates. (2) The CNTs suspension was sonicated (Selecta, 60 kHz, 200 W) for 60 min to yield mixtures of individualized CNTs and small-sized agglomerates (<3 μm).[19] (3) Diamond particles (Saint Gobain, <500 nm) were mixed together respecting the above-mentioned weight ratio and were sonicated for 30 min. (4) The CNT/diamond suspension was then dropped on a cylindrical mold and was placed onto a 0.22 μm pore size filter (Millipore). The buckypapers were finally obtained by vacuum filtration after coupling a rotary vane vacuum pump to a filter/Büchner funnel/Kitasato flask setup according to Figure 1a. For each CNT membrane, the amount of

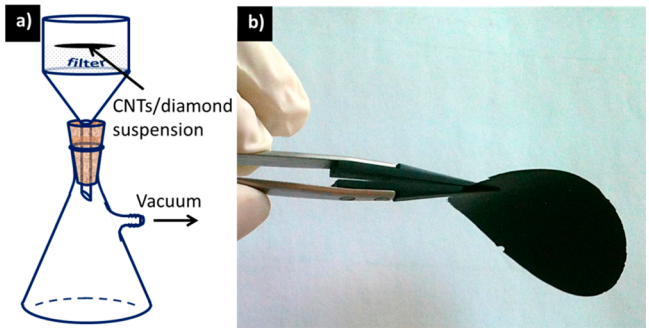

Figure 1. (a) Sketch of the experimental arrangement for CNTs filtration. (b) Ø 50 mm buckypaper.

filtrated suspension was estimated to reach thicknesses ranging from 30 to 150 μm, Figure 1b. (5) To improve a better CNT packing, buckypapers were uniaxially pressed with 0.1 MPa for 30 min. (6) Finally, the resulting membranes were dried in an oven at 80 °C for 15 min.

2.2. MPCVD NCD Growth. NCD diamond films were grown on the buckypaper substrates in a commercial MPCVD reactor (ASTeX PDS 18) using a water-cooled stage, as sketched in Figure 2a.

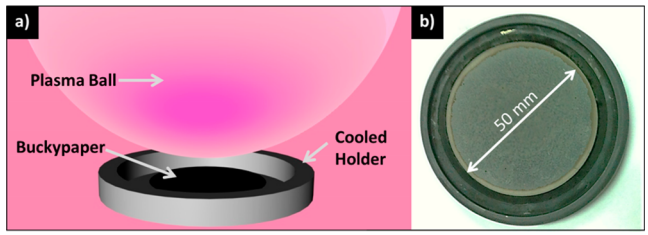

Figure 2. (a) Schematic illustration of the MPCVD NCD growth process. (b) NCD grown on CNT buckypaper placed on the molybdenum holder.

The growth process was achieved in a two-step routine. First, low microwave power was used (1600 W) to prevent CNT damage by the strong etching effect from the high atomic hydrogen concentration in the plasma ball. Once the CNTs were fully nucleated, the microwave power was increased to 3 kW for 1 h. In both steps, the ratio of the $H_2/CH_4/N_2$ gas mixture was fixed to 400/32/2 mL min^{-1}, and the total pressure varied from 60 to 105 Torr for low and high power, respectively. This method allows for uniform NCD growth on large area buckypaper substrates, Figure 2b.

2.3. Micro-Raman Analysis. The micro-Raman analysis was conducted in the backscattering configuration on a Jobin Yvon HR800 instrument (Horiba, Japan), using 1800 lines/mm grating and the 532 nm laser line from a Nd:YAG DPSS laser (Ventus, Laser Quantum, U.K.). For the Rayleigh rejection, an edge filter fits this equipment

allowing Raman acquisition from 50 cm^{-1}. A 50× objective (spot size ~ 3 μm, numeric aperture = 0.75, Olympus, Japan) was used to focus the laser light onto the sample and to collect the backscattered Raman radiation to be detected by a Peltier cooled (223 K) CCD sensor. The spectrometer was operated in the confocal mode, setting the iris to 250 μm and the integration time to 20 s.

2.4. Nanoindentation Bending Tests. CNT/NCD structures as well as pristine buckypaper disks were bend-tested using a diamond nanoindenter with a nominal edge radius of 150 nm attached to a fully calibrated nanohardness tester (TTX-NHT, CSM Instruments). The measurements were accomplished with the following constant parameters: applied force of 3 mN, loading and unloading rates of 20 mN/min, and acquisition rate of 10 Hz.

Circular samples of pristine CNT buckypapers as well as NCD coated ones were prepared with a thickness h and were placed in a circular holder with a 1.25 mm radius hole (a) in its center, as described in the scheme of Figure 3. The load/stroke response of the

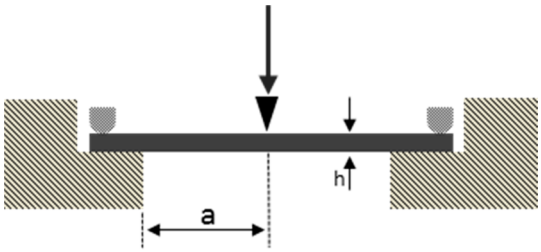

Figure 3. Schematic illustration of the performed bend testing.

sample was recorded under the bending regime, and the Young's modulus of the structures was estimated according to the following equation:[20]

$$\delta_t = \frac{3a^2(1-\upsilon^2)P}{4\pi E h^3} + \sqrt[3]{\frac{9P^2}{16RE_r^2}} \quad (1)$$

where υ is the Poisson's ratio, E_r is the reduced Young's modulus, E is the Young's modulus, P is the load applied by a spherical tip with radius R on the center of the sample (also center of the hole), and δ_t is the total displacement.

2.5. Electrical Properties. Electrical measurements both on pristine and NCD coated buckypapers were performed in order to evaluate the effect of the upper diamond film on the overall electrical resistivity. For this task, standard four-point measurements were conducted to assess the in-plane resistivity, while the two-point probe method was applied to ascertain the transverse one, a voltage having been applied across the samples.

The expected in-plane highly resistive behavior of the upper NCD film exceeded the measuring range of the equipment, and therefore, no accurate data were acquired in this case.

3. RESULTS AND DISCUSSION

CNT buckypapers with a diameter up to 50 mm were successfully produced by vacuum filtration, from MWCNTs suspensions. With this technique, the formation of flexible substrates with high uniformity in thickness along its width was achieved. The thickness of the buckypaper membranes was tailored by controlling the amount of CNT suspension used in each run, without compromising the overall uniformity. CNTs with carboxylic groups were selected for this application once they allowed a better dispersion, thus preventing the formation of CNT agglomerates. During the filtration process, when diamond particles were used, the membranes tended to bend during the drying process. To circumvent this effect, uniaxial pressing (0.1 MPa) was applied in that stage permitting the production of flat samples.

To guarantee diamond nucleation and growth, thus achieving a closed film, diamond particles were comixed with the CNT dispersion, keeping the buckypaper typical morphology. In fact, cross-sectional low-magnification images of the starting CNT buckypaper depicted a lamellar morphology with good uniformity in thickness, Figure 4a and b.

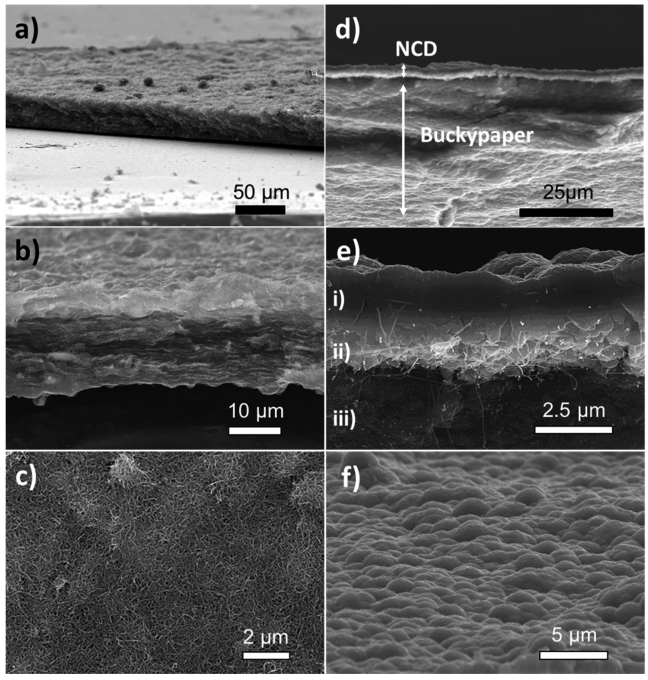

Figure 4. (a–c) SEM micrographs of the buckypapers produced by suspension filtration of CNTs and diamond particles at different magnifications. (d, e) Cross section images of the grown NCD film on CNT buckypaper. (i) NCD grown film, (ii) transition zone, (iii) buckypaper substrate. (f)Top view of the NCD grown film.

Additionally, the surface topography exhibits microscaled roughness with positive and negative protrusions capable of promoting mechanical interlock with the upper NCD film. Taking a higher magnification overview of the sample, a uniform distribution and high entanglement of the CNTs is patent, Figure 4c.

The diamond particles impregnated within the buckypaper act as nucleation sites in the early stages of CVD growth, promoting a fast formation of a diamond upper layer that constitutes an effective diffusion barrier. This helps to preserve the sp^2 carbon phases (CNTs) underneath the diamond growing film, protecting them from the aggressive etching by the plasma-produced atomic hydrogen. The resulting material consists in a well-defined CNT/NCD layered structure. The cross section images of the NCD coated buckypaper, Figure 4d and e, clearly depict three distinct layers. From top to bottom, they correspond to (i) the NCD film, (ii) a diamond/CNT transition zone, and (iii) the buckypaper substrate, as illustrated in Figure 4e.

In a first stage, when the diamond growth conditions are attained, the diamond particles present near the buckypaper surface start to overgrow until they eventually coalesce, like in a standard nucleation process on a pretreated surface. This leads to an NCD closed film, fully coating the buckypaper surface and evidencing traces of a ballas-like morphology, Figure 4f.[21] Until the NCD film closes, while there is still gas availability

beneath the diamond growing film, sp^3 carbon phases nucleate on the CNTs outer walls thickening the tubes in diameter. This zone gradually changes in morphology, from CNTs to NCD, where an intimate link is observed, thus explaining the visible merging of thicker tubes within the NCD matrix, Figure 5. In

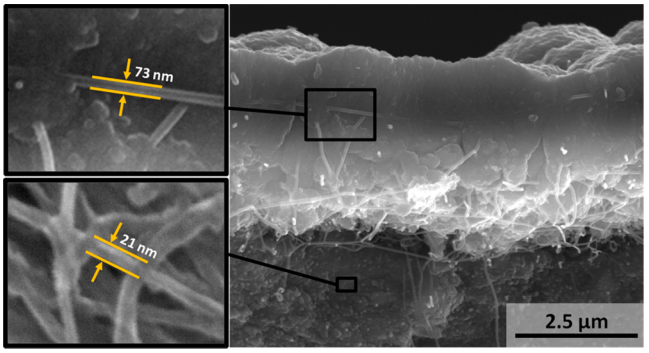

Figure 5. SEM micrographs comparing the CNTs diameter of the pristine buckypaper with those mixed within the NCD matrix after MPCVD growth.

fact, the overgrown embedded nanotubes present more than a 3-fold increase in diameter compared with the starting ones, insets of Figure 5. The CNTs within the NCD film help improve the mechanical interlock between both materials, therefore reinforcing the interface connection. This suggests that a synergistic integration of properties from each carbon allotrope is possible, foreseeing interesting potential applications.

The μ-Raman analysis was performed to structurally characterize the CNT/NCD multilayer structure. With this purpose, a cross-sectional analysis was undertaken in order to assess each layer. Pristine buckypapers displayed the typical MWCNT Raman features, namely, the D, G, and D′ bands, Figure 6a. Under the 532 nm wavelength laser excitation, the D

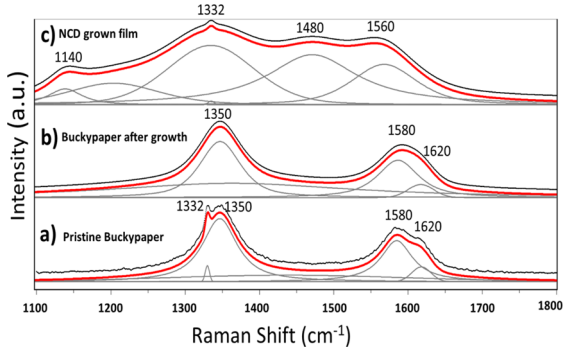

Figure 6. Raman spectra (solid lines) of the carbon structure in three different zones: (a) Pristine buckypaper, (b) buckypaper after NCD growth, (c) and NCD grown on the top of the CNT buckypaper. Dash lines correspond to the sum of the fitted Gauss−Lorentz curves (dash−dot lines).

band appeared at ∼1350 cm^{-1}, the G band at ∼1580 cm^{-1}, and the D′ shoulder at ∼1620 cm^{-1}. In this spectrum, the diamond contribution was patent in the form of a small peak at 1332 cm^{-1}, since the laser spot (∼1 μm) was purposely placed in order to include diamond particles embedded in the buckypaper. After deposition, although the D/G ratio intensity slightly diminished, an obvious increase was observed in the full width at half-maximum (fwhm) for both D (56−65 cm^{-1}) and G (51−66 cm^{-1}) bands because of a higher amorphization degree induced by the highly reactive hydrogen plasma attack. However, no significant changes of the D/G intensity ratio were found, confirming the preservation of the nanotubes that constitute the buckypaper. These data were obtained by fitting the spectra with Gauss−Lorentz curves after linear background removal, using the Labspec software. For the outer diamond layer, Figure 6c, the distinctive signatures of NCD were observed, namely, the diamond peak at ∼1332 cm^{-1}, the D band at ∼1350 cm^{-1}, the TPA (transpolyacetylene) bands at ∼1140 cm^{-1} and ∼1480 cm^{-1}, and the G band around 1560 cm^{-1}.

Because the above-mentioned integration between the CNT and NCD phases anticipates a good linkage, an attempt to measure the impact of the NCD coating on the mechanical properties of the buckypaper membranes was undertaken. Therefore, nanoindentation experiments under the bending regime, Figure 7a and b, were conducted in a modified setup of a nanohardness tester, as described in the Experimental Section . Using a similar approach to that of Ashrafi et al.,[20] the Young's modulus of the final structure was estimated and compared with that of the pristine buckypaper, according to eq 1. For Young's modulus calculations, the total displacement after a 10 s hold before unloading was considered. According to the literature, a Poisson's ratio of 0.275 was adopted for the pristine buckypaper, corresponding to the median value of the reported interval,[22,23] while 0.18 was considered for the NCD/buckypaper hybrid, corresponding to that of the dominating NCD phase.[24−26] To confirm the expected bending response for indentations at the center of the hole, a set of standard indentations (out of the hole) were also performed for comparison. While standard indentations on NCD coated samples evidenced strong hysteresis because of indenter penetration and general sink-in deformation, Figure 8, those performed at the hole center (bending) revealed total recovery, the hysteresis being practically absent as depicted in Figure 7b.

Interestingly, during loading, the bending mode and the standard indentations register very similar responses until a penetration depth of ∼200 nm is attained. After this point, they behave differently: while standard indentations register a slope decrease, the bending ones display a continuous slope up to the maximum load, totally recovering during unloading and showing a negligible final deformation.

Conversely, standard indentations terminate with a final deformation of ∼220 nm, corresponding to the transition point. This may indicate that a critical deformation underneath the NCD layer is produced for penetrations deeper than 200 nm. This way, Young's modulus of ∼300 and ∼0.3 GPa is estimated for the CNT/NCD structures and the uncoated buckypaper, respectively. This dramatic change reveals that the bending response of the diamond-coated buckypaper is mainly dominated by the upper NCD layer. However, eq 1 requires elastic isotropic behavior in order to extract Young's modulus estimations by bend testing, which is the case of NCD. In fact, Bi et al.[27] reported that since NCD grows in a randomly noncolumnar mode, it can be considered as an isotropic material.

Similarly to the mechanical properties, the electrical resistivity was dramatically influenced by the coating with NCD. In fact, the strong anisotropy in resistivity showed by the pristine buckypapers was hugely enhanced after a resistive thin layer of nanocrystalline diamond was deposited. For the

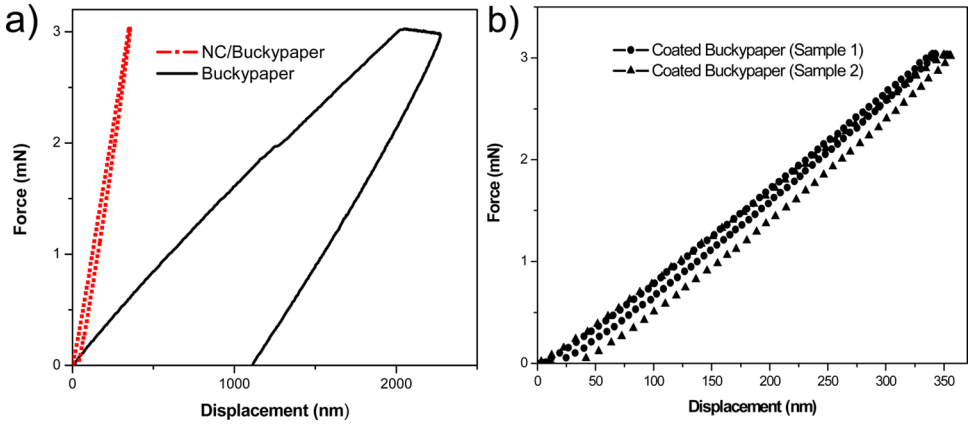

Figure 7. (a) Bend testing of NCD coated and uncoated buckypapers. (b) Load displacement of NCD coated buckypapers tested to a maximum load of 3 mN.

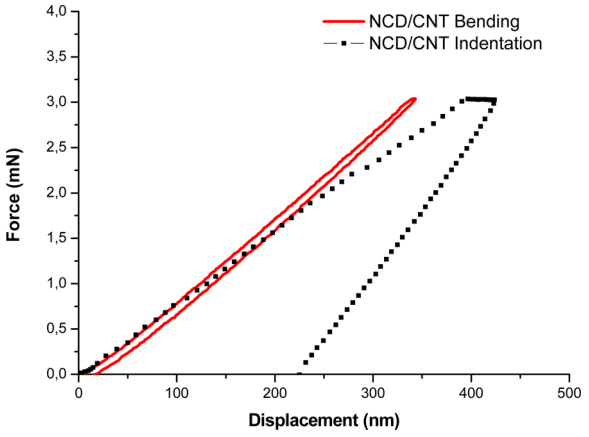

Figure 8. Load displacement of NCD/buckypaper in bending regime and on standard indentation with a maximum load of 3 mN.

uncoated buckypapers, the transverse to in-plane resistivity ratio was ~10^5, while for the coated ones it increased to more than 10^9 (see Table 1).

Table 1. Resistivity Values of the Pristine and NCD Coated Buckypapers

	Pristine Buckypaper	NCD coated Buckypaper
Young's modulus (GPa)	0.3	300
in-plane resistivity (Ω.cm)	1.39×10^{-1}	$>10^6$
transverse resistivity (Ω.cm)	6.18×10^2	8.13×10^5

Values of 1.39×10^{-2} Ω.cm were found for the CNT buckypaper using the four-point probe method. Cross-sectional and transverse measurements revealed that the NCD film dominates the electrical behavior with an estimated resistivity of 8.13×10^5 Ω.cm. Still, pristine buckypapers present high resistivity (6.18×10^2 Ω.cm) to transverse current flow, given the preferential orientation of the CNTs in the buckypaper structure. Because of the high aspect ratio of this material, in the filtration process, the CNTs remain lying horizontally on the final structure forming a strong anisotropic material, also visible in Figure 4 c. As expected, once MWCNTs yield high/ballistic conductivity only along its axis, whereas transverse conductivity is limited by the contact resistance between the CNTs outer walls, the transverse resistivity is much higher, about 3 orders of magnitude.[28,29]

One can think of a set of interesting applications for the here presented material, namely, those related with MEMS. Because high-frequency vibrations can be achieved due to the high Young's modulus, a resonator can be designed to take advantage of the highly porous and conductive buckypaper layer that moves along with the NCD coating. This way, a capacitive hybrid device (NCD is an insulator while CNTs are conductive) can be imagined, transforming mechanical motion into high-frequency electric signals. For example, if an upper buckypaper layer is functionalized to immobilize a specific chemical species, its attachment to the surface will induce changes in the electrical conductivity or resonance frequency of the device, thus producing readable data as a sensor. Cold cathodes, electrodes for cyclic voltammetry, and capacitors are also possible applications that could benefit from well-interconnected CNT/NCD bilayers.

4. CONCLUSIONS

Uniform CNT buckypapers were successfully and reproducibly produced to be used as free-standing substrates for diamond deposition. NCD closed films of high quality were grown on the buckypapers after a fast nucleation, without compromising the lower CNTs structure. A strong coupling of both phases was effectively achieved in an intimate mixture of both materials, consisting in a hybrid structure of CNTs mixed within the NCD matrix at the interface region.

Bending tests in a modified nanohardness tester showed that the NCD coated buckypapers mainly produced an elastic response with negligible hysteresis, in opposition to pristine buckypapers that evidenced strong plastic deformation. An increase of 4 orders of magnitude on the Young's modulus (0.3 to 300 GPa) was achieved by coating the buckypaper with NCD using the MPCVD technique, showing that the bending response is dominated by the upper NCD film.

The electrical behavior of the final structures was also investigated. Although the pristine buckypaper exhibits intrinsically higher/lower in-plane/transverse electrical conductivity, the NCD film strongly increases (3 orders of magnitude) the transverse resistivity of the hybrid structure, resulting in an enhanced anisotropic behavior.

Given the intimate linkage between both carbon phases, their high Young's modulus, and the possibility of controlling the thickness of each layer, the NCD coated buckypapers can be

easily tailored to meet specific requirements in selected applications such as MEMS.

■ ASSOCIATED CONTENT

Supporting Information

This material is available free of charge via the Internet at http://pubs.acs.org.

■ AUTHOR INFORMATION

Corresponding Author

*Tel: +351 234 370 296. E-mail: tiago.holz@ua.pt.

Notes

The authors declare no competing financial interest.

■ ACKNOWLEDGMENTS

The financial funding from the FCT projects NANO-CARBOMEMS PTDC/CTM-NAN/117284/2010 is gratefully acknowledged. N. F. Santos acknowledges financial support from the FCT PhD grant SFRH/BD/90017/2012. PEst-C/CTM/LA0025/2013-14 is gratefully acknowledged.

■ REFERENCES

(1) Dresselhaus, M. S. Fifty Years in Studying Carbon-Based Materials. *Phys. Scr.* **2012**, *T146*, 014002.

(2) Dresselhaus, M.; Endo, M. In *Carbon Nanotubes*; Dresselhaus, M., Dresselhaus, G., Avouris, P., Eds.; Springer: Berlin, 2001; Chapter 2, pp 11−28.

(3) Lee, D. H.; Kim, J. E.; Han, T. H.; Hwang, J. W.; Jeon, S.; Choi, S.-Y.; Hong, S. H.; Lee, W. J.; Ruoff, R. S.; Kim, S. O. Versatile Carbon Hybrid Films Composed of Vertical Carbon Nanotubes Grown on Mechanically Compliant Graphene Films. *Adv. Mater.* **2010**, *22*, 1247−1252.

(4) Yang, L.; Yang, Q.; Zhang, C.; Li, Y. S. Vertically Aligned Carbon Nanotubes/Diamond Double-layered Structure for Improved Field Electron Emission Stability. *Thin Solid Films* **2013**, *549*, 42−45.

(5) Tzeng, Y.; Chen, W. L.; Wu, C.; Lo, J.-Y.; Li, C.-Y. The Synthesis of Graphene Nanowalls on a Diamond Film on a Silicon Substrate by Direct-current Plasma Chemical Vapor Deposition. *Carbon* **2013**, *53*, 120−129.

(6) Vlasov, I.; Lebedev, O. I.; Ralchenko, V. G.; Goovaerts, E.; Bertoni, G.; Van Tendeloo, G.; Konov, V. I. Hybrid Diamond-Graphite Nanowires Produced by Microwave Plasma Chemical Vapor Deposition. *Adv. Mater.* **2007**, *19*, 4058−4062.

(7) Li, Y. S.; Hirose, A. Controlled Synthesis of Diamond and Carbon Nanotubes on Ni-base Alloy. *Appl. Surf. Sci.* **2008**, *255*, 2251−2255.

(8) Fernandes, A. J. S.; Pinto, M.; Neto, M. A.; Oliveira, F. J.; Silva, R. F.; Costa, F. M. Nano Carbon Hybrids from the Simultaneous Synthesis of CNT/NCD by MPCVD. *Diamond Relat. Mater.* **2009**, *18*, 160−163.

(9) Varshney, D.; Ahmadi, M.; Guinel, M.-F.; Weiner, B.; Morell, G. Single-step Route to Diamond-nanotube Composite. *Nanoscale Res. Lett.* **2012**, *7*, 1−6.

(10) Sellam, A.; Miska, P.; Ghanbaja, J.; Barrat, S. Catalytic Growth of Carbon Nanowires on Composite Diamond/Silicon Substrates. *Appl. Surf. Sci.* **2014**, *288*, 702−709.

(11) Hébert, C.; Ruffinatto, S.; Eon, D.; Mermoux, M.; Gheeraert, E.; Omnès, F.; Mailley, P. A Composite Material Made of Carbon Nanotubes Partially Embedded in a Nanocrystalline Diamond Film. *Carbon* **2013**, *52*, 408−417.

(12) Shankar, N.; Glumac, N. G.; Yu, M.-F.; Vanka, S. P. Growth of Nanodiamond/Carbon-nanotube Composites with Hot Filament Chemical Vapor Deposition. *Diamond Relat. Mater.* **2008**, *17*, 79−83.

(13) Zhang, L.; Zhang, G.; Liu, C.; Fan, S. High-Density Carbon Nanotube Buckypapers with Superior Transport and Mechanical Properties. *Nano Lett.* **2012**, *12*, 4848−4852.

(14) Varga, M.; Kotlar, M.; Vretenar, V.; Izak, T.; Ledinsky, M.; Michalka, M.; Skakalova, V.; Kromka, A.; Vesely, M. HFCVD Growth of Various Carbon Nanostructures on SWCNT Paper Controlled by Surface Treatment. *Phys. Status Solidi B* **2012**, *249*, 2399−2403.

(15) Yang, Q.; Yang, S.; Xiao, C.; Hirose, A. Transformation of Carbon Nanotubes to Diamond in Microwave Hydrogen Plasma. *Mater. Lett.* **2007**, *61*, 2208−2211.

(16) Bogus, A.; Gebeshuber, I. C.; Pauschitz, A.; Roy, M.; Haubner, R. Micro- and Nanomechanical Properties of Diamond Film with Various Surface Morphologies. *Diamond Relat. Mater.* **2008**, *17*, 1998−2004.

(17) Liao, M.; Koide, Y. Carbon-Based Materials: Growth, Properties, MEMS/NEMS Technologies, and MEM/NEM Switches. *Crit. Rev. Solid State Mater. Sci.* **2011**, *36*, 66−101.

(18) Rodrigues, J.; Fernandes, A. J. S.; Mata, D.; Holz, T.; Carvalho, R. G.; Fath Allah, R.; Ben, T.; Gonzalez, D.; Silva, R. F.; da Cunha, A. F.; Correia, M. R.; Alves, L. C.; Lorenz, K.; Neves, A. J.; Costa, F. M.; Monteiro, T. ZnO Micro/Nanocrystals Grown by Laser Assisted Flow Deposition. *Proc. SPIE* **2014**, *8898*, 89871F/1−89871F/22.

(19) Mata, D.; Oliveira, F. J.; Ferro, M.; Gomes, P. S.; Fernandes, M. H.; Lopes, M. A.; Silva, R. F. Multifunctional Carbon Nanotube/Bioceramics Modulate the Directional Growth and Activity of Osteoblastic Cells. *J. Biomed. Nanotechnol.* **2014**, *10*, 725−743.

(20) Ashrafi, B.; Das, K.; Faive, R.; Hubert, P.; Vengallatore, S. Measuring the Elastic Properties of Freestanding Thick Films Using a Nanoindenter-Based Bending Test. *Exp. Mech.* **2012**, *52*, 371−378.

(21) Yang, T.-S.; Lai, J.-Y.; Cheng, C.-L.; Wong, M.-S. Growth of Faceted, Ballas-like and Nanocrystalline Diamond Films Deposited in CH4/H2/Ar MPCVD. *Diamond Relat. Mater.* **2001**, *10*, 2161−2166.

(22) Li, Y.; Kröger, M. A theoretical evaluation of the effects of carbon nanotube entanglement and bundling on the structural and mechanical properties of buckypaper. *Carbon* **2012**, *50*, 1793−1806.

(23) Hall, L. J.; Coluci, V. R.; Galvao, D. S.; Kozlov, M. E.; Zhang, M.; Dantas, S. O.; Baughman, R. H. Sign Change of Poisson's Ratio for Carbon Nanotube Sheets. *Science* **2008**, *320*, 504−507.

(24) Tanei, H.; Nakamura, N.; Ogi, H.; Hirao, M.; Ikeda, R. Unusual Elastic Behavior of Nanocrystalline Diamond Thin Films. *Phys. Rev. Lett.* **2008**, *100*.

(25) Tanei, H.; Tanigaki, K.; Kusakabe, K.; Ogi, H.; Nakamura, N.; Hirao, M. Stacking-fault structure explains unusual elasticity of nanocrystalline diamonds. *Appl. Phys. Lett.* **2009**, *94*, 041914.

(26) Mohr, M.; Caron, A.; Herbeck-Engel, P.; Bennewitz, R.; Gluche, P.; Brühne, K.; Fecht, H.-J. Young's modulus, fracture strength, and Poisson's ratio of nanocrystalline diamond films. *J. Appl. Phys.* **2014**, *116*, 124308.

(27) Bi, B.; Huang, W. S.; Asmussen, J.; Golding, B. Surface acoustic waves on nanocrystalline diamond. *Diamond Relat. Mater.* **2002**, *11*, 677−680.

(28) Zhang, J.; Jiang, D.; Peng, H.-X.; Qin, F. Enhanced Mechanical and Electrical Properties of Carbon Nanotube Buckypaper by in situ Cross-linking. *Carbon* **2013**, *63*, 125−132.

(29) Slobodian, P.; Riha, P.; Lengalova, A.; Svoboda, P.; Saha, P. Multi-wall Carbon Nanotube Networks as Potential Resistive Gas Sensors for Organic Vapor Detection. *Carbon* **2011**, *49*, 2499−2507.